Perturbative dynamics in the pseudocoherent phase of the spin-boson model

Jiarui Zeng [1] and Yao Yao [1,2,*]

[1]*Department of Physics, South China University of Technology, Guangzhou 510640, China*

[2]*State Key Laboratory of Luminescent Materials and Devices, South China University of Technology, Guangzhou 510640, China*

(Received 19 February 2024; revised 4 June 2024; accepted 27 June 2024; published 12 July 2024)

We propose a time-dependent perturbation theory to study a newly discovered pseudocoherent phase of the spin-boson model. Effectiveness of the method is confirmed by comparing its results with that calculated from the numerically exact quantum dynamics method, which exhibits good agreements. We then describe how an incoherent nature of the pseudocoherent phase emerges from explicit expressions of the proposed method, and properties of invariant time of extreme values and scaling of amplitudes resulting from a second-order approximation. Correction effects of higher-order terms are also discussed. In addition, we utilize trace distance to investigate non-Markovianity and influences of model parameters. We find propagations in the pseudocoherent phase are always non-Markovian because of bath-driving oscillations. The non-Markovianity shows different dependence on cutoff frequency of bosonic baths from coherent and incoherent phases, which can be applied for qualitative identifications of different dynamic phases in realistic detections.

DOI: 10.1103/PhysRevA.110.012212

I. INTRODUCTION

The spin-boson model has hitherto attracted great attention during the past several decades, because of its fundamental physics of describing a spin coupled to a thermal bath consisting of an infinite number of bosonic modes [1]. The model, known for its localized-delocalized phase transition [2,3], can be mapped from and to the Kondo model which describes the scattering of conduction electrons in a metal due to magnetic impurities [1,4–6]. Furthermore, there is also another transition, the so-called dynamic phase transition, in the spin-boson model [1]. This transition can be characterized with a crossover between a coherent phase and incoherent phase [7–10]. For weak spin-boson couplings, the propagations of the spin are in the coherent phase, exhibited as underdamped oscillating behaviors with determined coherence time. While the couplings increase, the oscillation crosses a critical point and becomes overdamped, leading to the incoherent decay. The coherent and incoherent features and their corresponding dynamic phase transition have been utilized into investigations of quantum computations and simulations considering a dissipative bath [11–14].

In spite of extensive applications such as in driven quantum systems [15,16], charge-transfer states [17,18], optical and electrical responses [19,20], and transfers of heat [21,22], there remain a number of open questions to be investigated concerning the spin-boson model. In a very recent work, a new pseudocoherent phase beyond the conventionally known coherent and incoherent phases is revealed by Otterpohl *et al.*, through demonstrations of several properties like bath-driving aperiodic oscillations [23]. Thanks to numerically exact quantum dynamics methods, the corresponding phase boundaries can be determined even considering complicated spin-boson couplings. In a later work conducted by the same group, the pseudocoherent properties under a super-Ohmic spectral density are also investigated with a pronounced nonmonotonous behavior observed [24]. In addition, the influences of different initial preparations of the bosonic bath on the dynamic phase diagram are also investigated [25]. These insightful works have provided profound understandings about the pseudocoherent phase.

Nevertheless, it requires more effort to comprehend the physical properties of the pseudocoherent phase, especially an intuitive perspective to view its underlying properties. It is noticed that the pseudocoherent phase occurs in the strong-coupling regime, and it is therefore practical to gain perspective by treating tunneling of the spin as a perturbation. In this sense, one can combine the quantum dynamics methods with the time-dependent perturbation theory for the studies of the model. On the basis of this idea, we investigate the propagations of the spin by deriving two perturbation expressions the effectiveness of which is confirmed by the quantum dynamics method. For the pseudocoherent phase, although it has been known that the phase is induced by the bosonic bath, it is still unclear how its properties result from the bath. We describe how the incoherent nature would emerge from the explicit expressions, which is observed in the previous calculations [23], and then reveal the origin of the bath-dependence properties of the aperiodic oscillations. Furthermore, we use a description based on trace distance to discuss topical but controversial non-Markovianity [26–28]. The pseudocoherent phase is often connected to this property [23], but further studies are required to find a well-defined criterion for its existence and quantitatively describe its degrees.

The rest of the paper is organized as follows. In Sec. II, we describe the spin-boson model and propose the

*Contact author: yaoyao2016@scut.edu.cn

time-dependent perturbation theory. To confirm the effectiveness of the proposed method, we compare its results with those calculated from a quantum dynamics method, multi-D_1 *Ansatz*, because the *Ansatz* and its variants have been proved as reliable tools for a number of physical and chemical models including the spin-boson model [25,29–35]. After the confirmations, we then discuss the corresponding physical properties in Sec. III. Finally, Sec. IV draws a conclusion.

II. METHODS

A. Model

The unbiased spin-boson model is adopted as ($\hbar = 1$)

$$H = -\frac{\Delta}{2}\sigma_x + \sum_q \omega_q b_q^\dagger b_q + \sigma_z \sum_q \frac{\kappa_q}{2}(b_q^\dagger + b_q). \quad (1)$$

Herein, Δ represents spin tunneling strength, and σ_x and σ_z are Pauli operators with $\sigma_z|\pm\rangle = \pm|\pm\rangle$. ω_q and κ_q are frequency and spin-boson coupling strength referring to the qth bosonic mode, respectively. b_q ($b_q^\dagger$) is a boson annihilation (creation) operator of the qth bosonic mode. It is known that the model can be characterized with a spectral density:

$$J(\omega) = \sum_q \kappa_q^2 \delta(\omega - \omega_q) = 2\alpha\omega_c^{1-s}\omega^s e^{-\omega/\omega_c}, \quad (2)$$

where α is the Kondo parameter and ω_c is the cutoff frequency. Moreover, s specifies the bosonic bath to sub-Ohmic ($s < 1$), Ohmic ($s = 1$), and super-Ohmic ($s > 1$) baths. In the present paper, we focus on the sub-Ohmic situation and propagations of the spin $\langle\sigma_z\rangle$ to discuss the properties of the pseudocoherent phase. The initial state of the model is adopted as $|\psi(0)\rangle = |+\rangle \otimes |0\rangle$ for a factorized condition and zero temperature of the bath unless specified otherwise, where $|0\rangle$ is the vacuum state of the bath. Furthermore, $J(\omega)$ is discretized by a nonlinear discretization procedure for comparisons between two dynamics methods, the time-dependent perturbation theory and multi-D_1 *Ansatz*, with a number of the bosonic modes adopted as $N_{\text{bath}} = 200$ [25,36].

B. Time-dependent perturbation theory

Because the pseudocoherent phase appears when the couplings are strong, we assume that the spin tunneling strength is small comparing with the bosonic-mode frequencies and the spin-boson couplings. We thus define a system term

$$H_0 = \sum_q \omega_q b_q^\dagger b_q + \sigma_z \sum_q \frac{\kappa_q}{2}(b_q^\dagger + b_q) \quad (3)$$

and perturbation term $H_1 = -\Delta\sigma_x/2$. Then the Hamiltonian can be transformed with the time-dependent perturbation theory. Specifically, in an interaction picture

$$H_1'(t) = U_0^{-1} H_1 U_0. \quad (4)$$

Herein, U_0 is an evolution operator of H_0 as follows:

$$U_0 = \exp\left(-i\sum_q \omega_q b_q^\dagger b_q t\right) \exp\left(\frac{\sigma_z}{2}\sum_q b_q^\dagger g_q(t) - \text{H.c.}\right) \quad (5)$$

with $g_q(t) = \kappa_q/\omega_q(1 - e^{i\omega_q t})$. It is not difficult to confirm that the separate form of U_0 satisfies the Schrödinger equation $i\partial_t U_0(t) = H_0 U_0(t)$ and leads $H_1'(t)$ to

$$H_1'(t) = -\frac{\Delta}{2}\sigma_x \cosh\left(\sum_q b_q^\dagger g_q(t) - \text{H.c.}\right) + \frac{i\Delta}{2}\sigma_y \sinh\left(\sum_q b_q^\dagger g_q(t) - \text{H.c.}\right). \quad (6)$$

Then propagations of the wave function and $\langle\sigma_z\rangle$ in the interaction picture are acquired as

$$\begin{aligned}|\psi'(t)\rangle &= U_1|\psi(0)\rangle \\ &= \sum_{n=0}^{N}(-i)^n \int_0^t dt_1 \int_0^{t_1} dt_2 \cdots \\ &\quad \times \int_0^{t_{n-1}} dt_n H_1'(t_1)H_1'(t_2)\cdots H_1'(t_n)|\psi(0))\rangle|_{N\to\infty}\end{aligned} \quad (7)$$

and

$$\begin{aligned}\langle\sigma_z\rangle &= \langle\psi(t)|\sigma_z|\psi(t)\rangle \\ &= \langle\psi'(t)|U_0^{-1}\sigma_z U_0|\psi'(t)\rangle \\ &= \langle\psi'(t)|\sigma_z|\psi'(t)\rangle,\end{aligned} \quad (8)$$

respectively. Herein, $|\psi(t)\rangle$ and $|\psi'(t)\rangle$ are states at time t in Schrödinger and interaction pictures, respectively, and U_0 can be canceled by its inverse which commutes with σ_z.

We notice U_1 can be truncated to finite terms. For the second-order approximation, N is chosen as 2 and then

$$\begin{aligned}\langle\sigma_z\rangle^{(2)} &\approx 1 - 2\text{Re}\int_0^t dt_1 \int_0^{t_1} dt_2 \langle\psi(0)|H_1'(t_1)H_1'(t_2)|\psi(0)\rangle \\ &\quad - \int_0^t d\tau_1 \int_0^t dt_1 \langle\psi(0)|H_1'(\tau_1)H_1'(t_1)|\psi(0)\rangle \\ &= 1 - \frac{\Delta^2}{2}\text{Re}\int_0^t dt_1 \int_0^{t_1} dt_2\, S(g(t_1), g(t_2)) \\ &\quad - \frac{\Delta^2}{4}\int_0^t d\tau_1 \int_0^t dt_1\, S(g(\tau_1), g(t_1)) \\ &= 1 - \Delta^2\text{Re}\int_0^t dt_1 \int_0^{t_1} dt_2\, S(g(t_1), g(t_2)).\end{aligned} \quad (9)$$

Herein, $S(g', g) = \exp[\sum_q g_q'^* g_q - (|g_q'|^2 + |g_q|^2)/2]$ is an overlap between two coherent states and the term with the coefficient Δ^4 has been neglected. To obtain Eq. (9), the following equation is utilized:

$$H_1'(t)|\pm\rangle = -\frac{\Delta}{2}\exp\left(\pm\sum_q b_q^\dagger g_q(t) \mp \text{H.c.}\right)|\mp\rangle. \quad (10)$$

For the coherent-state overlap, an analytic decay function in a pure-dephasing case with $\omega_c \to \infty$ has been obtained in

Ref. [10]. For finite ω_c, the decay functions read

$$\Gamma_1(t) = \int_0^\infty d\omega \, \frac{J(\omega)}{\omega^2}[1-\cos(\omega t)] = 2\alpha\Gamma(s-1)\left\{1 - \frac{\cos\left[(s-1)\arctan(\omega_c t)\right]}{[1+(\omega_c t)^2]^{(s-1)/2}}\right\} \quad (11)$$

and

$$\Gamma_2(t) = \int_0^\infty d\omega \, \frac{J(\omega)}{\omega^2}\sin(\omega t) = 2\alpha\Gamma(s-1)\frac{\sin\left[(s-1)\arctan(\omega_c t)\right]}{[1+(\omega_c t)^2]^{(s-1)/2}}, \quad (12)$$

where $\Gamma(s-1)$ is the gamma function, and Eq. (11) has the same form as that of the super-Ohmic situation [24]. With $\Gamma_1(t)$ and $\Gamma_2(t)$, we can acquire the coherent-state overlap which is written as

$$S(g(t_1), g(t_2)) = \exp\{-\Gamma_1(t_2-t_1) + i[\Gamma_2(t_2-t_1) + \Gamma_2(t_1) - \Gamma_2(t_2)]\}. \quad (13)$$

A similar treatment in Eq. (9) is also employed for the fourth-order approximation $N = 4$ to capture more properties of the pseudocoherent phase. In this context,

$$\begin{aligned}\langle\sigma_z\rangle^{(4)} \approx \langle\sigma_z\rangle^{(2)} &+ \frac{\Delta^4}{16}\int_0^t d\tau_1\int_0^{\tau_1} d\tau_2\int_0^t dt_1\int_0^{t_1} dt_2\, e^{\sum_q [g_q^*(\tau_2)-g_q^*(\tau_1)][g_q(t_2)-g_q(t_1)]} S(g(\tau_2), g(\tau_1))S(g(t_1), g(t_2)) \\ &+ \frac{\Delta^4}{8}\mathrm{Re}\int_0^t dt_1\int_0^{t_1} dt_2\int_0^{t_2} dt_3\int_0^{t_3} dt_4\, e^{\sum_q [g_q^*(t_1)-g_q^*(t_2)][g_q(t_4)-g_q(t_3)]} S(g(t_1), g(t_2))S(g(t_3), g(t_4)) \\ &+ \frac{\Delta^4}{8}\mathrm{Re}\int_0^t d\tau_1\int_0^t dt_1\int_0^{t_1} dt_2\int_0^{t_2} dt_3\, e^{\sum_q [g_q^*(\tau_1)-g_q^*(t_1)][g_q(t_3)-g_q(t_2)]} S(g(\tau_1), g(t_1))S(g(t_2), g(t_3)) \\ &= \langle\sigma_z\rangle^{(2)} + \frac{\Delta^4}{4}\mathrm{Re}\int_0^t d\tau_1\int_0^t dt_1\int_0^{t_1} dt_2\int_0^{t_2} dt_3\, e^{\sum_q [g_q^*(\tau_1)-g_q^*(t_1)][g_q(t_3)-g_q(t_2)]} S(g(\tau_1), g(t_1))S(g(t_2), g(t_3)). \end{aligned} \quad (14)$$

The above time-dependent perturbation theory has a similar form to the iteration expression of the noninteracting blip approximation (NIBA) derived from the path-integral influence functional method [1,37–39]. However, it should be noted the NIBA provides a more powerful way to describe the quantum dynamics of the spin-boson model using the integrodifferential equation [40]. Nevertheless, it is not the main purpose of this paper to find a more powerful method but to describe how the bosonic bath causes the physical properties of the pseudocoherent phase. These will be conducted after the confirmations of the reliability of the time-dependent perturbation theory in the next section.

C. Variational Davydov *Ansatz*

To confirm the effectiveness of the time-dependent perturbation theory, we here introduce the variational Davydov *Ansätze* for comparisons. As mentioned in the Introduction, the *Ansätze* have been demonstrated as reliable approaches for describing the spin-boson model and its dynamic phase transition. In the present paper, the multi-D_1 *Ansatz* is utilized with a superposition of multiple coherent states [29,30]:

$$|\varphi(t)\rangle = \sum_{i,n} A_{in}(t)\exp\left(\sum_q b_q^\dagger \beta_{inq}(t) - \mathrm{H.c.}\right)|n\rangle. \quad (15)$$

Herein, i is the index of multiplicity M of the coherent states and $n = \{\pm\}$ refers to the eigenstates of σ_z. In addition, $A_{in}(t)$ and $\beta_{inq}(t)$ are variational parameters determined by the Dirac-Frenkel time-dependent variational principle, $\delta\int_0^t L dt = 0$, with the Lagrangian L defined as

$$L = \langle\varphi(t)|\left(\frac{i}{2}\overrightarrow{\partial}_t - \frac{i}{2}\overleftarrow{\partial}_t - H\right)|\varphi(t)\rangle. \quad (16)$$

Then we can obtain equations of motion of the variational parameters:

$$\frac{d}{dt}\frac{\partial L}{\partial \dot{u}^*} - \frac{\partial L}{\partial u^*} = 0. \quad (17)$$

Given $u^* = A_{jn}^*$ and β_{jnp}^*, the equations of motion can be acquired:

$$\sum_i \left\{ i\left[\dot{A}_{in} - A_{in}\sum_q\left(\frac{\dot{\beta}_{inq}\beta_{inq}^*}{2} + \frac{\beta_{inq}\dot{\beta}_{inq}^*}{2} - \beta_{jnq}^*\dot{\beta}_{inq}\right)\right] - A_{in} \times \left[\sum_q \omega_q\beta_{jnq}^*\beta_{inq} + n\sum_q\frac{\kappa_q}{2}\left(\beta_{jnq}^* + \beta_{inq}\right)\right]\right\} S(\beta_{jn}, \beta_{in}) + \frac{\Delta}{2}\sum_i A_{im}S(\beta_{jn}, \beta_{im}) = 0, \quad (18)$$

$$\sum_i \Bigg\{ -i \Bigg[\dot{A}_{in}\beta_{inp} + A_{in}\dot{\beta}_{inp} - A_{in}\beta_{inp} \sum_q \left(\frac{\dot{\beta}^*_{inq}\beta_{inq}}{2} + \frac{\beta^*_{inq}\dot{\beta}_{inq}}{2} - \beta^*_{jnq}\dot{\beta}_{inq} \right) \Bigg] + \omega_p A_{in}\beta_{inp} + n\frac{\kappa_p}{2}A_{in} + A_{in}\beta_{inp} \Bigg[\sum_q \omega_q \beta^*_{jnq}\beta_{inq} + n\sum_q \frac{\kappa_q}{2}\left(\beta^*_{jnq} + \beta_{inq}\right) \Bigg] \Bigg\} S(\beta_{jn}, \beta_{in}) - \frac{\Delta}{2}\sum_i A_{im}\beta_{imp} S(\beta_{jn}, \beta_{im}) = 0. \tag{19}$$

Herein, $m = \{\mp, \text{if} n = \pm\}$. After obtaining the propagations of the *Ansatz*, the observable $\langle\sigma_z\rangle$ can be calculated as

$$\langle\sigma_z\rangle^{\mathrm{DA}} = \sum_{j,i,n} n A_{jn}(t) A_{in}(t) S(\beta_{jn}(t), \beta_{in}(t)). \tag{20}$$

For a factorized initial condition, $A_{1,+}(0) = 1$, $A_{1,-}(0) = 0$, and $\beta_{11q}(0) = \beta_{12q}(0) = 0$ (q refers to all the bosonic modes). Other parameters are $A_{in}(0) = 0$ and $\beta_{inq}(0) = 0$ ($i > 1$, $n = \{\pm\}$, and q refers to all the bosonic modes). The multiplicity $M = 8$ is adopted. In addition, initial random noise with $|\varepsilon_A| < 10^{-5}$ and $|\varepsilon_\beta| < 10^{-3}$ is added to the variational parameters to avoid singularity while solving the equations of motion [32].

III. RESULTS AND DISCUSSIONS

A. Comparisons with the multi-D_1 *Ansatz*

We first exhibit the effectiveness of the time-dependent perturbation theory for the pseudocoherent phase of the spin-boson model. Figure 1 compares $\langle\sigma_z\rangle^{(2)}$ with the counterparts acquired from the multi-D_1 *Ansatz* with different model parameters, α and s. For $s = 0.2$, there is a deviation of $\langle\sigma_z\rangle^{(2)}$ for a small Kondo parameter $\alpha = 0.6$, as depicted in Fig. 1(a). While $\alpha \geqslant 1.2$, the time-dependent perturbation theory provides reliable results in good agreement with the multi-D_1 *Ansatz*. The same conclusion is also obtained for the other s in Figs. 1(b) and 1(c). In addition, it is found that the larger s leads to less accurate results if α is small, reflected in a relative error

$$r_n = \left| \frac{\langle\sigma_z\rangle^{\mathrm{DA}} - \langle\sigma_z\rangle^{(n)}}{\langle\sigma_z\rangle^{\mathrm{DA}}} \right|_{t=t_{\mathrm{f}}} \tag{21}$$

in Fig. 1(d). Herein, r_n is calculated at the final time t_{f} which is shown in Figs. 1(a)–1(c). Therefore, the larger α and smaller s correspond to the stronger-coupling regime, leading to more accurate results.

Taking into account a further approximation, it is less demanding for $\langle\sigma_z\rangle^{(4)}$ to approach the accurate results, as exhibited in Fig. 2. For $s = 0.2$ in Fig. 2(a), the time-dependent perturbation theory is adequate to capture the propagations of the spin, even considering a small Kondo parameter $\alpha = 0.6$. In addition, we find that $\langle\sigma_z\rangle^{(4)}$ gives rise to a correction of the extreme value, and shifts it toward an earlier stage. α for acquiring reliable results is also reduced for the other s as shown in Figs. 2(c) and 2(d), and the relative error r_4 decreases by around one order of magnitude. Even for $\alpha = 0.6$ and $s = 0.8$, it is sufficient to describe the propagation

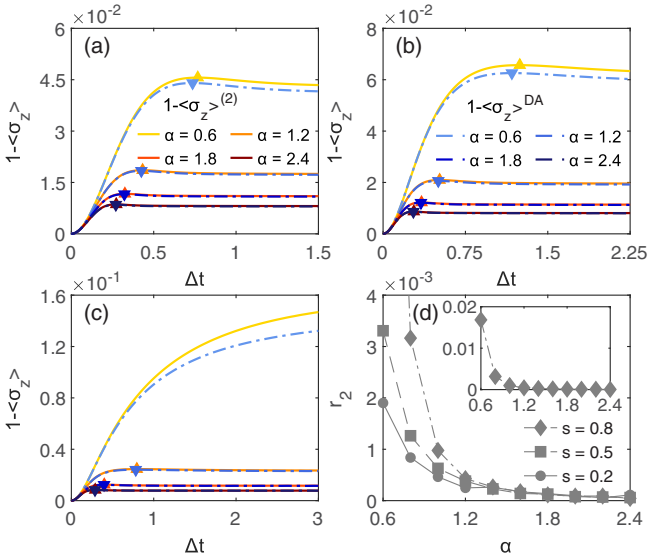

FIG. 1. Comparisons between $\langle\sigma_z\rangle^{(2)}$ (warm-color solid lines) and $\langle\sigma_z\rangle^{\mathrm{DA}}$ (cool-color dash-dotted lines), with the parameter (a) $s = 0.2$, (b) $s = 0.5$, and (c) $s = 0.8$. Other parameters are chosen as $\alpha = \{0.6, 1.2, 1.8, 2.4\}$, $\omega_c/\Delta = 10$, and $N_{\mathrm{bath}} = 200$. Extreme values of the lines are marked with triangles. (d) Relative errors r_2 with respect to α, calculated from the results in panels [(a)–(c)].

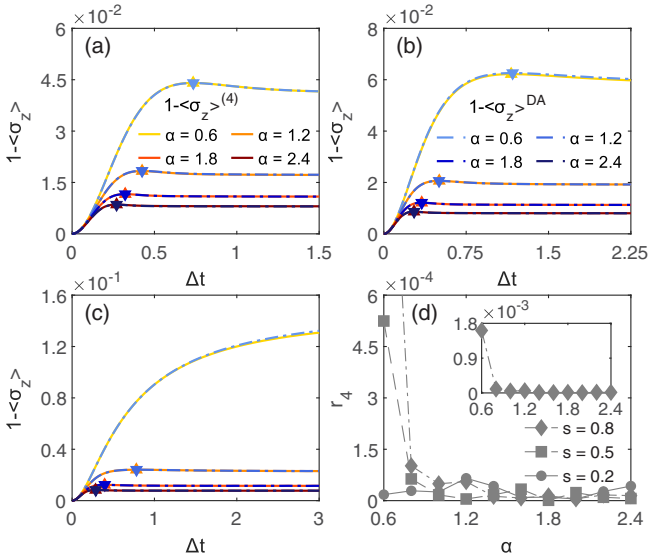

FIG. 2. Comparisons between $\langle\sigma_z\rangle^{(4)}$ (warm-color solid lines) and $\langle\sigma_z\rangle^{\mathrm{DA}}$ (cool-color dash-dotted lines), with the parameter (a) $s = 0.2$, (b) $s = 0.5$, and (c) $s = 0.8$. Other parameters are the same as Fig. 1. Extreme values of the lines are marked with triangles. (d) Relative errors r_4 with respect to α, calculated from the results in panels [(a)–(c)].

of the spin in the incoherent phase, in good agreement with the counterpart calculated from the multi-D_1 *Ansatz*. However, a rapid increase of r_4 is observed while the system crosses from the pseudocoherent to incoherent phase, i.e., α decreases from 0.8 to 0.6 for $s = 0.8$, indicating an inherent difficulty by means of the time-dependent perturbation theory.

B. Pseudocoherent properties

We now focus on the unique properties of the pseudocoherent phase, including an incoherent nature, invariant time of extreme values for large ω_c and its shift for small ω_c in the aperiodic oscillations, and scaling behaviors of oscillation amplitudes. These properties have been detected in computational results and attributed to the bosonic bath [23], and there remains a question of how they emerge from the complicated spin-boson couplings. We will show the pseudocoherent phase is the natural emergence of the second-order approximation of the time-dependent perturbation theory, the explicit expressions of which reveal the above properties.

The coherent phase is normally attributed to the drive of the tunneling term and leads the spin to a sinusoidal oscillating behavior, $\langle\sigma_z\rangle \sim \cos\Delta' t$, where Δ' is a renormalized parameter containing Δ. Despite observed oscillating behaviors, it is demonstrated that the pseudocoherent phase has an incoherent feature [23]. As exhibited in both Eqs. (9) and (14), the tunneling-induced oscillations are absent for the strong spin-boson couplings. Actually, the expressions explicitly reveal the incoherent nature of the pseudocoherent phase because the factors referring to Δ are time independent. The propagations of $\langle\sigma_z\rangle$ are instead contributed by a double integral of a coherent-state overlap $S(g', g)$ in Eq. (9) as well as a quadruple integral in Eq. (14), indicating the pure driving from the bosonic bath. If we exhibit $\langle\sigma_z\rangle^{(2)}$ and $\langle\sigma_z\rangle^{(4)}$ with respect to ω_c in Fig. 3(a), it would be found that the double and quadruple integrals reproduce the aperiodic oscillating behaviors of the propagations of the spin, depending on the frequency scale of the bosonic bath.

With increasing ω_c, the aperiodic oscillation of $\langle\sigma_z\rangle^{(2)}$ shows an invariant time scale as the extreme value always obeys $\omega_c t_x \sim$ const, as illustrated in Figs. 3(a) and 3(c). In addition, we also find that for the small ω_c the second-order approximation is not adequate to describe the propagations and hence requires the fourth-order correction, i.e., Eq. (14). Although the fourth-order term also has the invariant time of the extreme value as plotted in Fig. 3(b), once the correction is added to $\langle\sigma_z\rangle^{(2)}$, $\omega_c t_x$ is no longer a constant but shifts toward an earlier stage. It should be mentioned that the time shifts to the earlier rather than later stage because the fourth-order term significantly increases the derivative of $\langle\sigma_z\rangle^{(2)}$ while $\omega_c t \lesssim 5$, resulting in a new extreme value at the earlier stage at which $d\langle\sigma_z\rangle^{(2)}/dt < 0$, $d(\langle\sigma_z\rangle^{(4)} - \langle\sigma_z\rangle^{(2)})/dt > 0$, and their sum equals to zero. Moreover, the increasing ω_c also reduces the amplitudes of $\langle\sigma_z\rangle^{(2)}$ and $\langle\sigma_z\rangle^{(4)}$. To understand the behaviors of both $\omega_c t_x$ and the amplitude, it is helpful to perform the following variable substitutions for $\langle\sigma_z\rangle^{(2)}$:

$$\omega = \frac{\omega_c}{\omega_0}\omega', \quad \text{and} \quad t = \frac{\omega_0}{\omega_c}t', \tag{22}$$

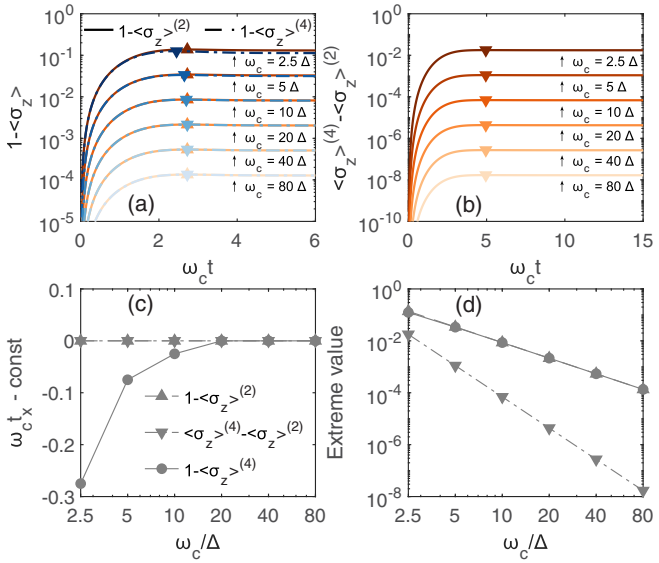

FIG. 3. (a) $\langle\sigma_z\rangle^{(2)}$ (warm-color solid lines) and $\langle\sigma_z\rangle^{(4)}$ (cool-color dash-dotted lines) and (b) fourth-order correction term with respect to $\omega_c t$. (c) Time and (d) amplitudes of extreme values of $\langle\sigma_z\rangle^{(2)}$ (dashed lines with triangles), $\langle\sigma_z\rangle^{(4)}$ (solid lines with dots), and the fourth-order terms (dash-dotted lines with triangles). Model parameters are chosen as $\alpha = 2.4$, $s = 0.2$, and $\omega_c/\Delta = \{2.5, 5, 10, 20, 40, 80\}$. In panel (c), each line has been shifted by a constant, to make $\omega_c t_x = 0$ for $\omega_c/\Delta = 80$. In panel (d), the lines referring to $\langle\sigma_z\rangle^{(2)}$ and $\langle\sigma_z\rangle^{(4)}$ overlap each other.

where ω_0 is a constant. Then the double integral can be transformed to

$$\int_0^t dt_1 \int_0^{t_1} dt_2\, S(g(t_1), g(t_2)) = \frac{\omega_0^2}{\omega_c^2}\int_0^{t'} dt_1' \int_0^{t_1'} dt_2'\, S\left(g\left(\frac{\omega_0}{\omega_c}t_1'\right), g\left(\frac{\omega_0}{\omega_c}t_2'\right)\right) \tag{23}$$

with the changed exponent of the coherent-state overlap exemplified as

$$\Gamma_1(t_2 - t_1) = 2\alpha\Gamma(s-1)\left\{1 - \frac{\cos\left[(s-1)\arctan(\omega_0\tilde{t}')\right]}{[1 + (\omega_0\tilde{t}')^2]^{(s-1)/2}}\right\}. \tag{24}$$

Herein, $\tilde{t}' = t_2' - t_1'$. In this sense, different spectral density $J(\omega)$ can be renormalized with an invariant effective cutoff frequency ω_0, leading $\langle\sigma_z\rangle^{(2)}$ to have (1) the invariant time of the extreme value $t_x' \sim \omega_c t_x \sim$ const and (2) the scalable amplitude with $1 - \langle\sigma_z\rangle^{(2)} \sim \omega_c^{-2}$. Similarly, the amplitude of the fourth-order correction term scales with $\sim\omega_c^{-4}$. In Figs. 3(c) and 3(d), we depict $\omega_c t_x$ and the amplitude of the extreme values with respect to ω_c, finding good agreements with the above discussions.

The above discussions reveal that ω_c can determine the scaling of the truncated terms and accordingly the effectiveness of the time-dependent perturbation theory. For the small ω_c, it is not sufficient to describe the propagations $\langle\sigma_z\rangle$ only with the truncated terms because those higher-order terms have significant contributions. For the large ω_c, on the other hand, the higher-order terms exhibit a rapid decrease toward

zero. The propagations of the spin thus can be described with $\langle\sigma_z\rangle^{(2)}$ and exhibit themselves as the pseudocoherent oscillations. However, it should be mentioned that the scaling depending on ω_c is not always established for the small α. It is found for $s \gtrsim 0.45$ that the coherent phase remains unchanged for an infinite ω_c, while for $s \lesssim 0.45$ the phase might become the pseudocoherent or incoherent phase. Detailed discussions can be also found in Refs. [3,23,41].

C. Non-Markovianity

To study the non-Markovianity of the pseudocoherent phase, we here utilize a quantitative measurement based on trace distance. Different from previous studies which focus on the (super-)Ohmic spectral density [42–47], we are interested in the sub-Ohmic case in the present paper. The trace distance between two states of the spin-boson model is defined as [48,49]

$$\mathcal{D}(t) = \tfrac{1}{2}\mathrm{Tr}|\rho_1(t) - \rho_2(t)|, \tag{25}$$

where the modulus of an operator A reads $|A| = \sqrt{A^\dagger A}$, and $\rho_1(0)$ and $\rho_2(0)$ can be chosen as all possible pairs of initial states. It has been demonstrated that the decrease and increase of $\mathcal{D}(t)$ can describe an information loss and backflow between the spin and bath, and for the latter case the propagations of the spin are defined to be non-Markovian due to memory effects [47,48]. Then the degree of the non-Markovianity can be acquired as

$$\mathcal{N} = \max_{\rho_1(0),\rho_2(0)} \int_{\dot{\mathcal{D}}(t)>0} dt\, \dot{\mathcal{D}}(t), \tag{26}$$

which should be maximized over pairs of the initial states [50]. In addition, $\dot{\mathcal{D}}(t) = d\mathcal{D}(t)/dt$ and the integral refers to the information backflow from the bosonic bath to the spin. It has been demonstrated that the optimal pairs leading to the maximum $\mathcal{N}$ must lie on the boundary of space of physical states and must be orthogonal [51]. This means, for a spin, the optimized pairs should be on the surface of the Bloch sphere:

$$|\psi_1(0)\rangle = \left(\cos\frac{\theta}{2}|+\rangle + e^{i\phi}\sin\frac{\theta}{2}|-\rangle\right)\otimes|0\rangle \tag{27}$$

and

$$|\psi_2(0)\rangle = \left(\sin\frac{\theta}{2}|+\rangle - e^{i\phi}\cos\frac{\theta}{2}|-\rangle\right)\otimes|0\rangle, \tag{28}$$

where $0 \leqslant \theta \leqslant \pi$ and $0 \leqslant \phi \leqslant 2\pi$. Therefore, calculations of the trace distance can be expressed as [47]

$$\mathcal{D}(\theta,\phi,t) = \frac{1}{2}\sqrt{\sum_{i=\{x,y,z\}}(\langle\sigma_i\rangle_1 - \langle\sigma_i\rangle_2)^2}. \tag{29}$$

In the Appendix, we derive the specific expressions of the trace distance. For a special situation $|\psi_1(0)\rangle = |+\rangle\otimes|0\rangle$ and $|\psi_2(0)\rangle = |-\rangle\otimes|0\rangle$, it can be written as

$$\mathcal{D}(0,0,t) = \sqrt{(\langle\sigma_z\rangle)^2 + \left(\frac{1}{\Delta}\frac{\partial}{\partial t}\langle\sigma_z\rangle\right)^2}. \tag{30}$$

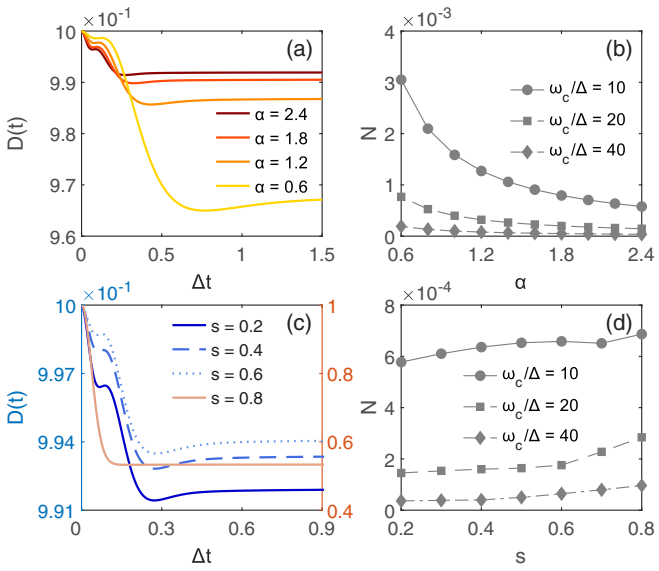

FIG. 4. (a) Trace distance $\mathcal{D}(t)$ and (b) degree of the non-Markovianity $\mathcal{N}$ with different α and $s = 0.2$. (c) $\mathcal{D}(t)$ and (d) $\mathcal{N}$ with different s and $\alpha = 2.4$. The cutoff frequencies are adopted as $\omega_c/\Delta = 10$ (a), (c) and $\{10, 20, 40\}$ (b), (d).

$\langle\sigma_z\rangle$ is calculated given $|\psi(0)\rangle = |+\rangle\otimes|0\rangle$ and its derivative refers to $\langle\sigma_y\rangle$. It is not difficult to know

$$\dot{\mathcal{D}}(0,0,t) = \frac{\partial}{\partial t}\langle\sigma_z\rangle\left(\langle\sigma_z\rangle + \frac{1}{\Delta^2}\frac{\partial^2}{\partial t^2}\langle\sigma_z\rangle\right)\mathcal{D}^{-1}(0,0,t). \tag{31}$$

Therefore, $\mathcal{D}(0,0,t)$ must possess the same extreme values as $\langle\sigma_z\rangle$. For the pseudocoherent phase, $\langle\sigma_z\rangle$ propagates with an aperiodic oscillation, leading $\mathcal{D}(0,0,t)$ to the increase and thus information backflow. Because $\mathcal{N}$ is greater than or equal to the integral of the information backflow of $\mathcal{D}(0,0,t)$, $\mathcal{N}$ is always nonzero and the propagations of the spin in the pseudocoherent phase always possess the non-Markovian feature.

In Fig. 4, we show $\mathcal{N}$ and corresponding $\mathcal{D}(t)$ acquired from the second-order approximation which allows us to perform the integrals within a time interval from $\omega_c t = 0$ to 50. We first focus on $\mathcal{D}(t)$ with different α in Fig. 4(a). It is found that $\mathcal{D}(t)$ always decreases from $\mathcal{D}(0) = 1$ corresponding to the initial trace distance between two initial states, and then exhibits two slow information backflows. Because of the localized feature, $\mathcal{D}(t)$ gradually saturates and approaches a finite value instead of zero. If increasing α, the information backflow of $\mathcal{D}(t)$ would be reduced, exhibited as the amplitudes of the aperiodic oscillations are reduced. This phenomenon is also reflected in the degree of the non-Markovianity in Fig. 4(b), as $\mathcal{N}$ exhibits a rapid decrease with increasing α. In addition, we find that $\mathcal{N}$ would be reduced while increasing ω_c, which is relevant to the frequency scaling of the bosonic bath as discussed in previous subsection. The dependence is very different from that of the coherent and incoherent phases, because $\mathcal{N}$ is enhanced while increasing ω_c for the former case and rigorous zero for the latter [47]. Therefore, the degree of the non-Markovianity is an applicable measurement as a qualitative identification of the different dynamic phases in realistic detections.

If changing s with fixed α, the non-Markovianity shows nonmonotonous behaviors. In Fig. 4(c), it is also found that the trace distance $\mathcal{D}(t)$ corresponding to $\mathcal{N}$ is reduced with small and increasing s. However, $\mathcal{D}(t)$ exhibits dramatic changes while $s = 0.8$, because the optimal pair of the initial states changes. In Fig. 4(d), it can be seen that the change of $\mathcal{N}$ is nonmonotonous. This phenomenon might be due to the complicated interplays between the aperiodic oscillations and exponential decays, as the former factor promotes the bath-driving information backflow and the latter one reduces it. Similarly, the increasing ω_c reduces $\mathcal{N}$ due to the scaling of the bosonic bath.

IV. CONCLUSIONS

In this paper, we have utilized the time-dependent perturbation theory to study the pseudocoherent properties of the spin-boson model. By regarding the tunneling of the spin as a perturbation, a method is derived to acquire the propagations of the spin and intuitive perspectives. We first compare its results with the counterparts calculated from the multi-D_1 *Ansatz*, confirming the reliability of the time-dependent perturbation theory. It is also found that larger α and smaller s refer to stronger spin-boson couplings, leading to more reliable results of the perturbative dynamics. After the confirmations, we describe how the pseudocoherent properties emerge from the second-order approximation given by the time-dependent perturbation theory, including the incoherent nature, invariant time of the extreme values, and scaling of the amplitudes. The correction effects of the fourth-order term are also discussed. The pseudocoherent phase also induces distinctive behaviors of the non-Markovianity which have not been studied based on the trace distance in the previous works. It is found that the propagations of the spin are always non-Markovian because of the aperiodic oscillations. The influences of the model parameters are also discussed, as the information backflow would be reduced with the increasing Kondo parameter. Changing s leads to the nonmonotonous results of both the trace distance and degree of the non-Markovianity. Moreover, the increasing cutoff frequency would reduce the degree of the non-Markovianity, which is different from the results of the coherent and incoherent phases and can be applied as a qualitative identification for the dynamic phases.

Our efforts may be extended for further studies of the pseudocoherent phase. For example, a resemblance has been found between two phase boundaries of the coherent and pseudocoherent phases, as well as under- and overdamping properties in a pure-dephasing model considering the super-Ohmic spectral density [24]. We notice that the second-order approximation given by the time-dependent perturbation theory has a similar form to the decay function in a pure-dephasing model, which might be relevant to the aforementioned resemblance of the phase boundaries. However, the topic is beyond our present scope in this paper, and it also requires hard treatments due to the inherent difficulty of describing the small Kondo parameter. Nevertheless, we believe our efforts can provide useful help for future studies.

ACKNOWLEDGMENT

This work was supported by the National Natural Science Foundation of China (Grants No. 12374107 and No. 11974118).

APPENDIX: DERIVATIONS OF THE TRACE DISTANCE

For an arbitrary pair of the pure and orthogonal initial states $|\psi_1(0)\rangle$ and $|\psi_2(0)\rangle$, the expectation of the Pauli operator σ_z for the first state can be acquired as

$$\begin{aligned}\langle\sigma_z\rangle_1 = \langle\psi_1(0)|e^{iHt}\sigma_z e^{-iHt}|\psi_1(0)\rangle &= \cos^2\frac{\theta}{2}\langle+,0|e^{iHt}\sigma_z e^{-iHt}|+,0\rangle + \sin^2\frac{\theta}{2}\langle-,0|e^{iHt}\sigma_z e^{-iHt}|-,0\rangle \\ &\quad + e^{i\phi}\cos\frac{\theta}{2}\sin\frac{\theta}{2}\langle+,0|e^{iHt}\sigma_z e^{-iHt}|-,0\rangle + e^{-i\phi}\cos\frac{\theta}{2}\sin\frac{\theta}{2}\langle-,0|e^{iHt}\sigma_z e^{-iHt}|+,0\rangle \\ &= \cos^2\frac{\theta}{2}\langle+,0|e^{iHt}\sigma_z e^{-iHt}|+,0\rangle + \sin^2\frac{\theta}{2}\langle-,0|\sigma_x^2 e^{iHt}\sigma_x^2\sigma_z\sigma_x^2 e^{-iHt}\sigma_x^2|-,0\rangle \\ &\quad + \frac{e^{i\phi}\sin\theta}{2}\langle+,0|e^{iHt}\sigma_z e^{-iHt}|-,0\rangle + \frac{e^{-i\phi}\sin\theta}{2}\langle-,0|\sigma_x^2 e^{iHt}\sigma_x^2\sigma_z\sigma_x^2 e^{-iHt}\sigma_x^2|+,0\rangle. \end{aligned} \tag{A1}$$

With $\tilde{H} = \sigma_x H \sigma_x$, the expression can be further simplified to be

$$\begin{aligned}\langle\sigma_z\rangle_1 &= \cos^2\frac{\theta}{2}\langle+,0|e^{iHt}\sigma_z e^{-iHt}|+,0\rangle - \sin^2\frac{\theta}{2}\langle+,0|e^{i\tilde{H}t}\sigma_z e^{-i\tilde{H}t}|+,0\rangle + \frac{e^{i\phi}\sin\theta}{2}\langle+,0|e^{iHt}\sigma_z e^{-iHt}|-,0\rangle \\ &\quad - \frac{e^{-i\phi}\sin\theta}{2}\langle+,0|e^{i\tilde{H}t}\sigma_z e^{-i\tilde{H}t}|-,0\rangle \\ &= \cos^2\frac{\theta}{2}\langle+,0|e^{iHt}\sigma_z e^{-iHt}|+,0\rangle - \sin^2\frac{\theta}{2}\langle+,0|e^{iHt}\sigma_z e^{-iHt}|+,0\rangle + \frac{e^{-i\phi}\sin\theta}{2}\langle+,0|e^{iHt}\sigma_z e^{-iHt}|-,0\rangle \\ &\quad - \frac{e^{-i\phi}\sin\theta}{2}\langle+,0|e^{iHt}\sigma_z e^{-iHt}|-,0\rangle \\ &= \cos\theta\langle+,0|e^{iHt}\sigma_z e^{-iHt}|+,0\rangle + i\sin\phi\sin\theta\langle+,0|e^{iHt}\sigma_z e^{-iHt}|-,0\rangle \\ &= \cos\theta\langle+,0|e^{iHt}\sigma_z e^{-iHt}|+,0\rangle - \sin\phi\sin\theta\langle+,0|e^{iHt}\sigma_y e^{-i\tilde{H}t}|+,0\rangle. \end{aligned} \tag{A2}$$

The above simplifications are established because $\tilde{H}$ gives rise to the same reduced dynamics of the spin as that induced by H [47]. In addition, the expectation of σ_y considering the first initial state is

$$\langle\sigma_y\rangle_1 = \cos\theta\langle+,0|e^{iHt}\sigma_y e^{-iHt}|+,0\rangle + \sin\phi\sin\theta\langle+,0|e^{iHt}\sigma_z e^{-i\tilde{H}t}|+,0\rangle. \tag{A3}$$

For those terms referring to σ_y, they can be obtained as

$$\begin{aligned}\langle+,0|e^{iHt}\sigma_y e^{-iHt}|+,0\rangle &= \frac{i}{2}\langle+,0|e^{iHt}[\sigma_x,\sigma_z]e^{-iHt}|+,0\rangle \\ &= -\frac{1}{\Delta}\langle+,0|e^{iHt}[iH,\sigma_z]e^{-iHt}|+,0\rangle \\ &= -\frac{1}{\Delta}\frac{\partial}{\partial t}\langle+,0|e^{iHt}\sigma_z e^{-iHt}|+,0\rangle,\end{aligned} \tag{A4}$$

and because

$$\begin{aligned}\langle+,0|e^{iHt}\sigma_z e^{-i\tilde{H}t}|+,0\rangle &= -\frac{i}{2}\langle+,0|e^{iHt}[\sigma_x,\sigma_y]e^{-i\tilde{H}t}|+,0\rangle \\ &= \frac{1}{\Delta}\langle+,0|e^{iHt}(iH\sigma_y - \sigma_y i\tilde{H})e^{-i\tilde{H}t}|+,0\rangle \\ &= \frac{1}{\Delta}\frac{\partial}{\partial t}\langle+,0|e^{iHt}\sigma_y e^{-i\tilde{H}t}|+,0\rangle\end{aligned} \tag{A5}$$

we have

$$\langle+,0|e^{iHt}\sigma_y e^{-i\tilde{H}t}|+,0\rangle = \Delta\int_0^t d\tau\langle+,0|e^{iH\tau}\sigma_z e^{-i\tilde{H}\tau}|+,0\rangle. \tag{A6}$$

Thus we have obtained two expectations of the Pauli operators considering the first initial state. For the second initial state, it can be easily acquired that $\langle\sigma_z\rangle_2 = -\langle\sigma_z\rangle_1$ and $\langle\sigma_y\rangle_2 = -\langle\sigma_y\rangle_1$.

Furthermore, $\langle\sigma_x\rangle_{1,2}$ can be calculated as

$$\begin{aligned}\langle\sigma_x\rangle_{1,2} &= \langle+,0|e^{iHt}\sigma_x e^{-iHt}|+,0\rangle - (-1)^{1,2}\cos\phi\sin\theta\langle+,0|e^{iHt}\sigma_x e^{-iHt}|-,0\rangle \\ &= \langle+,0|e^{iHt}\sigma_x e^{-iHt}|+,0\rangle - (-1)^{1,2}\cos\phi\sin\theta\langle+,0|e^{iHt}e^{-i\tilde{H}t}|+,0\rangle.\end{aligned} \tag{A7}$$

Finally, we obtain the specific expression of the trace distance for the spin-boson model:

$$\begin{aligned}\mathcal{D}(\theta,\phi,t) = \Bigg[&\left(\cos\theta\langle+,0|e^{iHt}\sigma_z e^{-iHt}|+,0\rangle - \sin\phi\sin\theta\Delta\int_0^t d\tau\langle+,0|e^{iH\tau}\sigma_z e^{-i\tilde{H}\tau}|+,0\rangle\right)^2 \\ &+\left(\frac{\cos\theta}{\Delta}\frac{\partial}{\partial t}\langle+,0|e^{iHt}\sigma_z e^{-iHt}|+,0\rangle - \sin\phi\sin\theta\langle+,0|e^{iHt}\sigma_z e^{-i\tilde{H}t}|+,0\rangle\right)^2 \\ &+(\cos\phi\sin\theta\langle+,0|e^{iHt}e^{-i\tilde{H}t}|+,0\rangle)^2\Bigg]^{1/2}.\end{aligned} \tag{A8}$$

This expression allows us to calculate all the terms only with the second-order time-dependent perturbation theory and fixed initial state $|\psi(0)\rangle = |+,0\rangle$.

[1] A. J. Leggett, S. Chakravarty, A. T. Dorsey, M. P. A. Fisher, A. Garg, and W. Zwerger, Dynamics of the dissipative two-state system, Rev. Mod. Phys. **59**, 1 (1987).

[2] A. Winter, H. Rieger, M. Vojta, and R. Bulla, Quantum phase transition in the sub-Ohmic spin-boson model: Quantum Monte Carlo study with a continuous imaginary time cluster algorithm, Phys. Rev. Lett. **102**, 030601 (2009).

[3] A. W. Chin, J. Prior, S. F. Huelga, and M. B. Plenio, Generalized polaron ansatz for the ground state of the sub-Ohmic spin-boson model: An analytic theory of the localization transition, Phys. Rev. Lett. **107**, 160601 (2011).

[4] S. Chakravarty, Quantum fluctuations in the tunneling between superconductors, Phys. Rev. Lett. **49**, 681 (1982).

[5] A. J. Bray and M. A. Moore, Influence of dissipation on quantum coherence, Phys. Rev. Lett. **49**, 1545 (1982).

[6] A. Kopp and K. LeHur, Universal and measurable entanglement entropy in the spin-boson model, Phys. Rev. Lett. **98**, 220401 (2007).

[7] F. B. Anders, R. Bulla, and M. Vojta, Equilibrium and nonequilibrium dynamics of the sub-Ohmic spin-boson model, Phys. Rev. Lett. **98**, 210402 (2007).

[8] P. Nalbach and M. Thorwart, Ultraslow quantum dynamics in a sub-Ohmic heat bath, Phys. Rev. B **81**, 054308 (2010).

[9] D. Kast and J. Ankerhold, Persistence of coherent quantum dynamics at strong dissipation, Phys. Rev. Lett. **110**, 010402 (2013).

[10] P. Nalbach and M. Thorwart, Crossover from coherent to incoherent quantum dynamics due to sub-Ohmic dephasing, Phys. Rev. B **87**, 014116 (2013).

[11] T. Palm and P. Nalbach, Dephasing and relaxational polarized sub-Ohmic baths acting on a two-level system, J. Chem. Phys. **150**, 234108 (2019).

[12] L. Magazzù, P. Forn-Díaz, R. Belyansky, J.-L. Orgiazzi, M. Yurtalan, M. R. Otto, A. Lupascu, C. Wilson, and M. Grifoni, Probing the strongly driven spin-boson model in a superconducting quantum circuit, Nat. Commun. **9**, 1403 (2018).

[13] J. Leppäkangas, J. Braumüller, M. Hauck, J.-M. Reiner, I. Schwenk, S. Zanker, L. Fritz, A. V. Ustinov, M. Weides, and M. Marthaler, Quantum simulation of the spin-boson model with a microwave circuit, Phys. Rev. A **97**, 052321 (2018).

[14] M. Abdi and M. B. Plenio, Analog quantum simulation of extremely sub-Ohmic spin-boson models, Phys. Rev. A **98**, 040303(R) (2018).

[15] G. Engelhardt, G. Platero, and J. Cao, Discontinuities in driven spin-boson systems due to coherent destruction of tunneling: Breakdown of the Floquet-Gibbs distribution, Phys. Rev. Lett. **123**, 120602 (2019).

[16] X. Cao, C. Wang, and D. He, Driving induced coherent quantum energy transport, Phys. Rev. B **108**, 245401 (2023).

[17] Y. Yao, Spin-boson theory for charge photogeneration in organic molecules: Role of quantum coherence, Phys. Rev. B **91**, 045421 (2015).

[18] Y. Yao, N. Zhou, J. Prior, and Y. Zhao, Competition between diagonal and off-diagonal coupling gives rise to charge-transfer states in polymeric solar cells, Sci. Rep. **5**, 14555 (2015).

[19] Y. Yan, L. Chen, J. Y. Luo, and Y. Zhao, Variational approach to time-dependent fluorescence of a driven qubit, Phys. Rev. A **102**, 023714 (2020).

[20] S. Dattagupta, Spin-boson model of quantum dissipation in graphene: Nonlinear electrical response, Phys. Rev. B **104**, 085411 (2021).

[21] D. Segal and A. Nitzan, Spin-boson thermal rectifier, Phys. Rev. Lett. **94**, 034301 (2005).

[22] D. Segal, Heat transfer in the spin-boson model: A comparative study in the incoherent tunneling regime, Phys. Rev. E **90**, 012148 (2014).

[23] F. Otterpohl, P. Nalbach, and M. Thorwart, Hidden phase of the spin-boson model, Phys. Rev. Lett. **129**, 120406 (2022).

[24] P. Nacke, F. Otterpohl, M. Thorwart, and P. Nalbach, Dephasing and pseudocoherent quantum dynamics in super-Ohmic environments, Phys. Rev. A **107**, 062218 (2023).

[25] L. Chen, Y. Yan, M. F. Gelin, and Z. Lü, Dynamics of the spin-boson model: The effect of bath initial conditions, J. Chem. Phys. **158**, 104109 (2023).

[26] H.-P. Breuer, E.-M. Laine, J. Piilo, and B. Vacchini, Colloquium: Non-Markovian dynamics in open quantum systems, Rev. Mod. Phys. **88**, 021002 (2016).

[27] I. de Vega and D. Alonso, Dynamics of non-Markovian open quantum systems, Rev. Mod. Phys. **89**, 015001 (2017).

[28] Á. Rivas, S. F. Huelga, and M. B. Plenio, Quantum non-Markovianity: Characterization, quantification and detection, Rep. Prog. Phys. **77**, 094001 (2014).

[29] Y. Zhao, K. Sun, L. Chen, and M. Gelin, The hierarchy of Davydov's Ansätze and its applications, WIREs Comput. Mol. Sci. **12**, e1589 (2022).

[30] Y. Zhao, The hierarchy of Davydov's Ansätze: From guesswork to numerically exact many-body wave functions, J. Chem. Phys. **158**, 080901 (2023).

[31] Y. Yao, L. Duan, Z. Lü, C.-Q. Wu, and Y. Zhao, Dynamics of the sub-Ohmic spin-boson model: A comparison of three numerical approaches, Phys. Rev. E **88**, 023303 (2013).

[32] L. Wang, L. Chen, N. Zhou, and Y. Zhao, Variational dynamics of the sub-Ohmic spin-boson model on the basis of multiple Davydov D_1 states, J. Chem. Phys. **144**, 024101 (2016).

[33] L. Chen, M. Gelin, and Y. Zhao, Dynamics of the spin-boson model: A comparison of the multiple Davydov D_1, $D_{1.5}$, D_2 Ansätze, Chem. Phys. **515**, 108 (2018).

[34] M. Jakučionis and D. Abramavičius, Temperature-controlled open-quantum-system dynamics using a time-dependent variational method, Phys. Rev. A **103**, 032202 (2021).

[35] M. Jakučionis and D. Abramavičius, Thermalization of open quantum systems using the multiple-Davydov-D_2 variational approach, Phys. Rev. A **107**, 062205 (2023).

[36] H. Wang and M. Thoss, Multilayer formulation of the multiconfiguration time-dependent Hartree theory, J. Chem. Phys. **119**, 1289 (2003).

[37] C. Aslangul, N. Pottier, and D. Saint-James, Spin-boson systems: Equivalence between the dilute-blip and the Born approximations, J. Phys. France **47**, 1657 (1986).

[38] H. Dekker, Noninteracting-blip approximation for a two-level system coupled to a heat bath, Phys. Rev. A **35**, 1436 (1987).

[39] A. Würger, Dissipative tunneling in insulators: Noninteracting blip approximation and beyond, Phys. Rev. Lett. **78**, 1759 (1997).

[40] U. Weiss, *Quantum Dissipative Systems* (World Scientific, Singapore, 2012).

[41] H. Wang and M. Thoss, From coherent motion to localization: Dynamics of the spin-boson model at zero temperature, New J. Phys. **10**, 115005 (2008).

[42] G. Clos and H.-P. Breuer, Quantification of memory effects in the spin-boson model, Phys. Rev. A **86**, 012115 (2012).

[43] H.-B. Chen, N. Lambert, Y.-C. Cheng, Y.-N. Chen, and F. Nori, Using non-Markovian measures to evaluate quantum master equations for photosynthesis, Sci. Rep. **5**, 12753 (2015).

[44] A. Rivas, Refined weak-coupling limit: Coherence, entanglement, and non-Markovianity, Phys. Rev. A **95**, 042104 (2017).

[45] M. Hinarejos, M.-C. Banuls, A. Pérez, and I. De Vega, Non-Markovianity and memory of the initial state, J. Phys. A **50**, 335301 (2017).

[46] A. Kurt and R. Eryigit, Noise-induced non-Markovianity, Phys. Rev. A **98**, 042125 (2018).

[47] S. Wenderoth, H.-P. Breuer, and M. Thoss, Non-Markovian effects in the spin-boson model at zero temperature, Phys. Rev. A **104**, 012213 (2021).

[48] H.-P. Breuer, E.-M. Laine, and J. Piilo, Measure for the degree of non-Markovian behavior of quantum processes in open systems, Phys. Rev. Lett. **103**, 210401 (2009).

[49] E.-M. Laine, J. Piilo, and H.-P. Breuer, Measure for the non-Markovianity of quantum processes, Phys. Rev. A **81**, 062115 (2010).

[50] H.-P. Breuer, Foundations and measures of quantum non-Markovianity, J. Phys. B **45**, 154001 (2012).

[51] S. Wißmann, A. Karlsson, E.-M. Laine, J. Piilo, and H.-P. Breuer, Optimal state pairs for non-Markovian quantum dynamics, Phys. Rev. A **86**, 062108 (2012).